EFFECT OF LENGTH-TO-DIAMETER RATIO ON CRITICAL HEAT FLUX IN POROUS-COATED TUBES

by

Sebiha YILDIZ *

Yildiz Technical University, Faculty of Mechanical Engineering
Department of Mechanical Engineering, Beşiktaş, Istanbul, Turkey

Original scientific paper
https://doi.org/10.2298/TSCI190426462Y

The critical heat flux occurring during upflow of boiling water in vertical smooth and porous-coated tubes were investigated experimentally. The experiments were performed at low pressures from 0.11-0.7 MPa and at mass fluxes from 100-400 kg/m^{2}s, with inlet subcoolings from 1-70 K. The experiments were carried out with four test sections, two of which were porous coated by sintering. The two tubes in each of the cases, porous and smooth, had the same geometries (L/D = 28.3, L/D = 38.75) to ensure a direct comparison of the measured data in the porous-coated tubes with those of the smooth tubes. In addition, the critical heat flux data for water in uniformly heated vertical porous-coated tubes were obtained from the literature. These experiments were conducted using two smooth and four inner porous-coated tubes (L/D = 14.1, L/D = 50) in the same experimental set-up used in the present study. In general, it was found that the critical heat flux decreased with an increase in the L/D ratio for both the smooth and porous-coated tubes. The effect of porous coating on critical heat flux can be positive, negative, or even neutral.

Key words: *L/D ratio, critical heat flux, smooth tube, porous-coated tube, vertical, water, upflow*

Introduction

The critical heat flux (CHF) is the highest amount of energy transferred per a specific surface area. It plays a crucial role in designing the heat transfer elements cooled with boiling liquids. Thus, researchers in the field are intrigued to find ways to maximize CHF rates without altering the existing operating conditions. The roughness of the tubes (finned, corrugated, and spirally fluted tubes; tubes with twisted tape and porous coating, *etc.*) are an efficient quality by which the CHF is enhanced. Apart from the internal surface geometry, the known geometric parameter that influences the CHF is the ratio of tube length to diameter (*L/D*).

Boyd [1] suggested that pressure, mass-flow, inlet subcooling, diameter, and heated length are the fundamental parameters influencing the CHF. According to Boyd [1], although many authors have stated values of *L/D* beyond which it does not affect CHF, it is not clear what this limiting value is or whether *L/D* is the appropriate parameter to characterize such an effect. Incropera and DeWitt [2] introduced the dimensionless hydrodynamic entry length for turbulent single-phase flow as $10 \leq L/D \leq 60$ and the dimensionless thermal entry length for

* Author's, e-mail: syildiz@yildiz.edu.tr

turbulent flow as L/D = 10. Celata *et al.* [3] experimentally investigated the influence of the geometric parameters of a tube on CHF under subcooled water-flow. Tube diameters ranged from 0.25 mm to 4 mm, and the tubes had a heated length ranging from 10 mm to 160 mm (L/D altering from 5 to 40). The results showed that the effect of the L/D on the CHF is insignificant for L/D values greater than 30, and the functional dependence between the CHF and L/D is not dependent on the mass flux. The CHF increased as the channel length decreased for L/D below 30. According to Tanase [4], lower threshold values for L/D are common for high flow and low exit qualities ($x < 0.1$), and higher threshold values are common for high exit qualities and low flow conditions. The influence of the heated length is far more important in the dryout-type CHF.

Collier *et al.* [5] provided evidence that the CHF decreases with increasing heated length for the fixed inlet conditions. Mastrullo *et al.* [6] studied saturated CHF in a rectangular multi micro-channel heat sink. The working fluids were R134a and the low global warming potential refrigerants R1234ze, R1234yf, and R32. Three different L/D ratios of 19, 27, and 44 were studied. At low mass flux (up to 351 kg/m^{2}s), CHF decreased when the L/D increased from 19 to 44. This tendency appears to be the opposite for higher mass flux (> 500 kg/m^{2}s). Sudo [7] also studied the effect of L/D on CHF. A systematic investigation of the characteristics of the CHF under high subcooling and high water velocity in short heated channels (L/D = 1, 6, 25, 40) was carried out. It was found that the effect of L/D on CHF was significant when L/D was less than about 20. According to Sudo [7], the reason for this is the increase in heat transfer coefficients at the entrance or the developing flow region of the single-phase forced-convection flow. Significantly high CHF measurements during subcooled flow boiling using water were carried out by Mudawar *et al.* [8]. The range of the tube diameters was 0.40 to 2.54 mm, and the heated L/D ratios were in the range of 2.4-34.1. In their study, there were mass fluxes of 5000-134000 kg/m^{2}s and pressures of 3.2-172.4 bars. The results of the study suggest that CHF increased with increasing mass flux, increasing the subcooling, decreasing the tube diameter, and decreasing the heated L/D ratio. Lee *et al.* [9] developed a CHF correlation using a correction factor from the L/D ratio. A value of L/D beyond which the length effect becomes small was defined as a threshold L/D value. The threshold value was not a constant because it changed according to other system parameters. A decrease in mass flux and an increase in quality raised the threshold L/D. Roday *et al.* [10] reviewed the CHF in mini- and micro-channels. They found that CHF increased with an increase in mass flux and decreased with an increase in the heated length. A threshold value of L/D = 150 was suggested by Wu *et al.* [11], after which L/D has no significant effect on saturated CHF.

It can be seen from the literature that there is disagreement about the threshold value of L/D. According to Boyd [1], despite this disagreement, the CHF increases with decreasing L/D. Furthermore, since the L/D limit is related directly to the flow development, this limit is not a constant, but is related to the flow parameters and fluid properties.

Many researchers have investigated CHF on a porous-coated surface [12-20]. Kovalev *et al.* [12] investigated CHF on a porous surface in an annular channel. The working fluid was water. They found that thin fine-pored coatings were more convenient. The improvement of CHF with porous coating was 3-4 times compared to a smooth surface. The CHF with a number of horizontal test sections was investigated by Leont`ev *et al.* [13]. The porous structure has capillary force, which thins out the laminar flow layer and intensifies the turbulence. Kovalev *et al.* [14] suggested that the small pores on the porous coating enable the liquid to penetrate the coating, and the vapor softens along the big channel. Kotov *et al.* [15]

found that the effect of the porous layers was dependent on the mass flux and the pressure. The CHF improved at a mass flux of 1500 kg/m^{2}s for pressures higher than 12 MPa and deteriorated at a mass flux of 1500 kg/m^{2}s for pressures lower than 12 MPa.

An investigation of the CHF during upflow in vertical tubes (*L/D* = 125) with and without porous coating with homogeneous heating was conducted by Zuev *et al.* [16]. For mass fluxes lower than 1500 kg/m^{2}s, a deterioration of the CHF was obtained, and an improvement of the CHF was obtained for mass fluxes higher than 1500 kg/m^{2}s when compared to the smooth tubes. The authors reported that the chronological development of the boiling crisis was slower in porous-coated tubes than in smooth tubes. Dawidowicz *et al.* [17] found that average heat transfer coefficient can be increased 5-6 times by applying a porous coating on the inside surface of a tube (*L/D* = 227.27, 250). An investigation of the effect of porous iron oxide coatings on the CHF in an upflow circular tube was conducted by Melnikov *et al.* [18]. The layer thickness was varied when compared to the smooth tubes; the thicker the layer, the greater the deterioration (up to 35%) was observed.

A majority of CHF experiments were performed at very high pressures or at very high mass fluxes. The results of the *L/D* effect on CHF provided in the literature are conflicting. Furthermore, there is no study in the literature on the *L/D* effect on CHF in porous-coated tubes. In this study, the effect of the *L/D* ratio on CHF was investigated not only in smooth tubes both also in porous-coated tubes. Moreover, the influence of sintered porous coatings on the CHF during upflow boiling was investigated for low mass fluxes and low pressures. This study involves two experimental CHF studies that were carried out using the same experimental test set-up and the same working fluid of water [19, 20]. In this study, *L/D* ratios were 14.11, 28.33, 38.75, and 50.

Experimental set-up and method

The experimental test loop is described in detail in [19, 20]. The experimental set-up consists of four main components: a water cycle, a directly heated test section, a power supply system for the test section, and a measuring data-acquisition system. The pressure transducers were calibrated with the aid of a precision measuring gauge with an accuracy of 0.1% of the full-scale value. The inlet and outlet temperatures of the test section are measured with a Pt-100 resistance thermometer of accuracy class A using a 4-wire technique. For the measurement of the volume flow, there are three flow meters, from 0.05 to 10 L per minute. The measuring error is 1-2% of the end value of the respective measuring range.

In the present study, two smooth and two internally porous-coated tubes were used for the CHF measurements. Each of the porous and smooth tubes had the same length and diameter in order to compare the measured data against each other. The porous coating was produced through sintering. This study also took into account the CHF data from the literature. Thus, the range of the *L/D* ratio was expanded from 14.11 to 50. The two smooth and four internally porous-coated tubes with an inside diameter of 9 mm were used by Stein [20] for CHF measurements. Each three tubes had the same length, and the two of three tubes were porous coated but differed in the parameters of the coating. This allowed for a direct comparison of the experimentally determined data. All of the tubes' characteristics are presented in tab. 1.

The porous coatings were examined by means of a SEM, and the layer thickness and porosity of the coating parameters were determined with the aid of micrographs and surface photographs of the porous layer at different points of the test sections [19].

Figure 1 shows the schematic structure of a test section and the burnout protection system. Two flanges were welded to each end of the tubes. The power supply units of a DC

Table 1. The characteristics of the test tubes

Reference	Tubes		D [mm]	L [mm]	L/D	Particle diameter d_p, [μm]	Layer thickness δ, [μm]	Porosity ε, [%]
Present study	Smooth	Inconel-600	6	170	28.33	–	–	–
	Porous coating (1)	Inconel-600	6	170	28.33	80-100	350	60-70
	Smooth	Steel	8	310	38.75	–	–	–
	Porous coating (2)	Steel	8	310	38.75	100-140	180	~50
[20]	Smooth	Inconel-600	9	127	14.11	–	–	–
	Porous coating (3)	Inconel-600	9	127	14.11	30-40	300	60-75
	Porous coating (4)	Inconel-600	9	127	14.11	60-80	300	60-75
	Smooth	Inconel-600	9	450	50	–	–	–
	Porous coating (3)	Inconel-600	9	450	50	30-40	300	60-75
	Porous coating (4)	Inconel-600	9	450	50	60-80	300	60-75

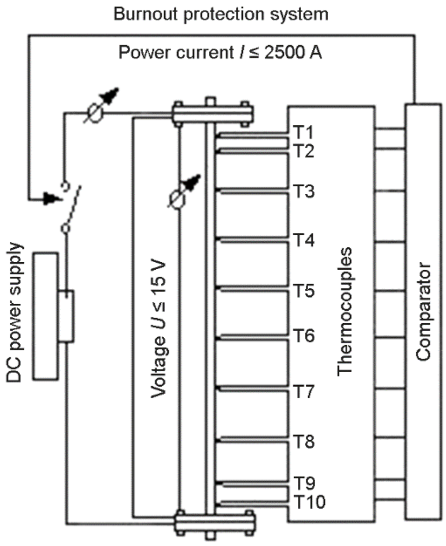

Figure 1. Scheme of the test section [19]

power supply (15 V, 2500 A) of the test section were mounted on the flanges so that the test section could be electrically heated directly and homogeneously. The test section was electrically isolated from the system. The voltage was measured directly at the test section, and the current was measured directly at the output of the power supply. The thermocouples (LKI 05/25, 0.5 mm outer diameter) were fixed on the outer tube walls to detect the wall temperature of the test sections. During the measurements, the heating power at the test section was carefully increased over time until the CHF occurred. To avoid thermal destruction of the heating surface (burnout), the signals from thermocouples were routed to digital comparators. The comparators were connected to the DC power supply of the test section to form a burnout protection system. If one of the thermocouple signals exceeds the value set on the comparator, this leads to a disconnection of the power supply. The entire test section was insulated to reduce heat losses to the surroundings.

Test program and evaluation of the results

Before each test, the circulating water was filtered for at least three hours, desalted, and degassed. The system was separated from the atmosphere for all CHF measurements. With manual control of the cooling capacity of the condenser, the system pressure was slowly increased. Once the intended system pressure was reached, manual control was switched over to automatic control. The pressure was regulated to ±2 kPa. Then, the mass flux and the inlet temperature of the test section were set. When the system stabilized, continuous measurement was started. With the function generator, the heat flux was increased linearly. The CHF was obtained using the following equation:

$$\dot{q}_{\mathrm{cr}} = \frac{IU}{\pi DL} \tag{1}$$

where $\dot{q}_{\mathrm{cr}}$ is the CHF, I – the current, U – the voltage, D – the inside diameter, and L – the length between the measuring points of the voltage of the test section. The voltage U and the current I were measured with an accuracy of ±0.5%. Considering additional error due to heat losses (estimated at ±1%), a measurement inaccuracy was included, and the CHF was determined to be ±4% [20].

Results and discussion

The CHF during the upflow of water was measured experimentally in vertical homogeneously heated tubes with and without porous coating. The CHF experimental parameter ranges for the present study and Stein's [20] study are given in tab. 2.

Table 2. General experimental conditions.

Reference	Pressure P, [MPa]	Mass flux G, [kgm^{-2}s^{-1}]	Inlet subcooling ΔT_{i}, [K]
Present study	0.11, 0.4, 0.7	100-400	1-70
[20]	0.12, 0.4, 0.7	50-300	15, 30, 50

Effect of the L/D ratio

The effect of the tube L/D ratio on the CHF is studied for the smooth and porous-coated tubes. In the following sections, $\dot{q}_{\mathrm{cr}}$ is the arithmetic mean of the repeated CHF measurements.

Different heated lengths with a constant diameter

The CHF data from study by Stein [20], which were obtained at a constant inner diameter of 9 mm for all six tubes (two smooth and four porous coated) with two different tube lengths of 0.127 m and 0.45 m, are presented here. The effect of L/D ratio on the CHF for a mass-flow of 100 kg/m^{2}s and at the fixed inlet subcooling of 30 K is presented for the smooth and porous-coated tubes in figs. 2 and 3, respectively. The CHF for smooth and porous-coated tubes increases with decreasing the heated length for all pressures. This behavior is similar to the results reported in the literature. For L/D = 14.11, the CHF at atmospheric pressure is lower than the one at elevated pressures for both smooth and porous-coated tubes. However, for L/D = 50, the pressure effect on CHF becomes insignificant. For smooth tubes,

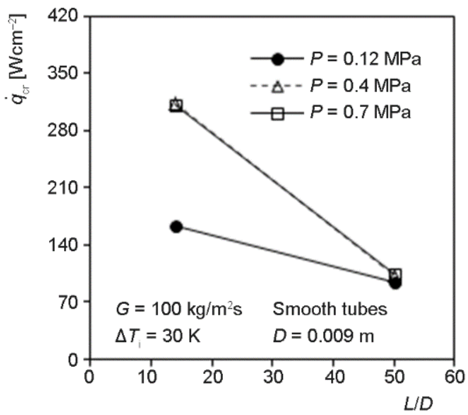

Figure 2. Effect of *L/D* ratio on the CHF at different pressures in the smooth tubes [20]

the effect of pressure on the CHF at high pressure does not appear. In fig. 3 at atmospheric pressure, for L/D = 14.11, the CHF for the coating (4) is higher than the one for the coating (3), which is vice versa at L/D = 50. As the pressure increases, there are no visible differences between the CHF values for the coating (3) and (4).

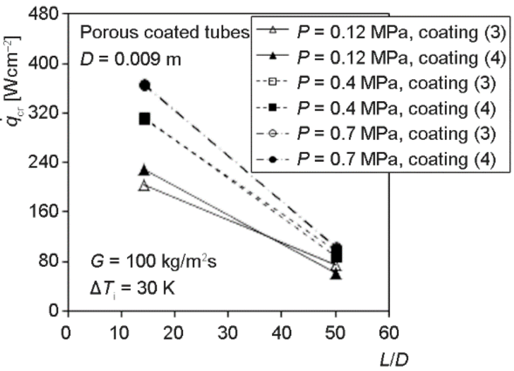

Figure 3. Effect of *L/D* ratio on the CHF at different pressures in porous-coated tubes [20]

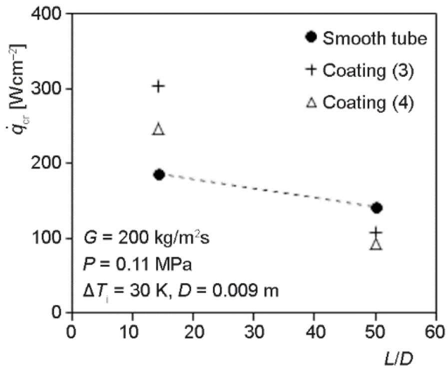

Figure 4. Comparison of the CHF in smooth and porous-coated tubes [20]

The effect of the porous coating on the CHF with an increase in L/D ratio is shown for the mass flux of 200 kg/m^{2}s at 0.11 MPa in fig. 4. The CHF on the porous coatings compared to smooth tube increased at L/D = 14.11. Moreover, the CHF for coating (3) is higher than the one for coating (4) at L/D = 14.11. However, at L/D = 50, there is a deterioration of the CHF for both porous coating (3) and (4) in fig. 4.

Different heated lengths with different diameters

It can be seen from figs. 5 and 6 that the CHF with and without porous coating decreases with increasing L/D ratio for the mass flux of 200 kg/m^{2}s. In fig. 5, there are two smooth tubes having different lengths and diameters. For each smooth tube, there is a porous-

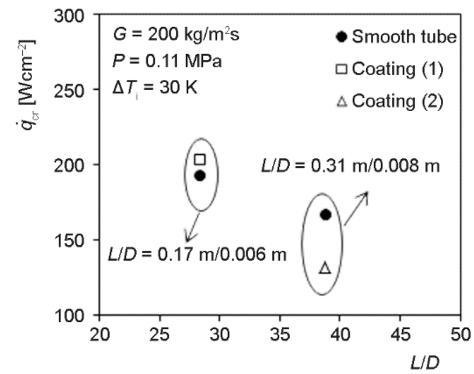

Figure 5. Comparison of the CHF in tubes with different heated lengths and different inside diameters with and without porous coatings at atmospheric pressure

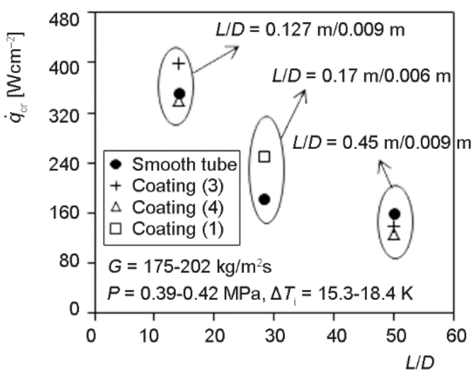

Figure 6. Comparison of the CHF in tubes with different heated lengths and different inside diameters with and without porous coatings at elevated pressure taking the data for *L/D* = 14.11 and 50 from [20]

coated tube with the same diameter and length, tab. 1. In fig. 5, at the atmospheric pressure for L/D = 28.33, the CHF with the coating (1) is slightly higher than the one in the smooth tube. However, at L/D = 38.75, deterioration occurs by using the coating (2). At about 0.4 MPa in fig. 6, for L/D = 14.11, with coating (3), there is an enhancement of CHF, whereas with coating (4) there is no visible effect. The CHF is higher with coating (1) compared to the smooth tubes at L/D = 28.33. However, for L/D = 50, there is a slight deterioration of CHF with the coating (3) and (4) compared to the smooth tubes.

Effect of mass flux, pressure, and inlet subcooling

The CHF ratio $\dot{q}_{\mathrm{cr,pr}}/\dot{q}_{\mathrm{cr}}$ is the ratio of the CHF in the porous-coated tube to the CHF in the smooth tube. Figures 7-10 show the CHF ratio *vs.* the mass flux at different pressures and different inlet subcoolings.

For the inlet subcooling of 20 K for L/D = 28.33, the CHF ratio against the mass flux is presented for different pressures in fig. 7. For the mass flux of 100 kg/m^{2}s, there is no visible effect of coating (1) on the CHF for all pressures. At atmospheric pressure, there is a deterioration of CHF, which is the maximum at the mass flux of 300 kg/m^{2}s. However, for the pressures of 0.4 and 0.7 MPa, the CHF ratio reaches a maximum value at the mass flux of 200 kg/m^{2}s, and then it starts to decrease. A maximum increase of the CHF by about 36% is seen at the mass flux of 200 kg/m^{2}s for the pressure of 0.4 MPa and the inlet subcooling of 20 K in fig. 7. The maximum improvement of the CHF with porous coating (1) in the present study was 41% for the mass flux of 200 kg/m^{2}s and the inlet subcooling of about 10 K at a pressure of 0.4 MPa, which was reported in [19].

Figure 8 shows that a slight positive effect of porous coating (1) is visible for the inlet subcooling of 70 K at L/D = 28.33 at the pressure of 0.4 MPa except for the mass flux of 200 kg/m^{2}s. There are negative effects for the other pressures. For L/D = 38.75, it was reported in [19] that the effect of porous coating (2) on the CHF is negative at atmospheric pressure. However, at the pressure of 0.7 MPa, the maximum improvement of CHF with porous coating (2) was about 19% for the mass flux of 100 kg/m^{2}s at the inlet subcooling of 30 K.

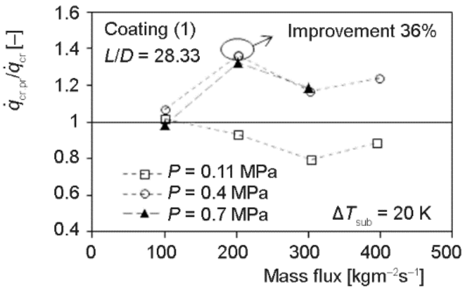

Figure 7. Effect of the mass flux on the CHF with porous coating (1) for the inlet subcooling of 20 K

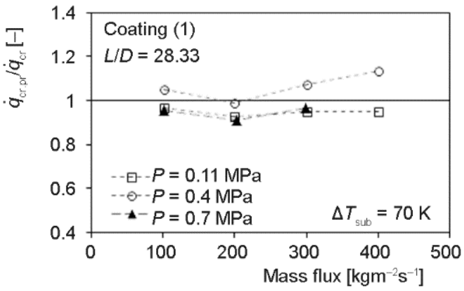

Figure 8. Effect of the mass flux on the CHF with porous coating (1) for the inlet subcooling of 70 K

For L/D = 14.11, the CHF measurements obtained by Stein [20] with porous coating (3) and (4) compared to the smooth tube are shown for the inlet subcooling of 15 K and 50 K in figs. 9 and 10, respectively. For the inlet subcooling of 15 K at the pressure of 0.12 MPa, the CHF ratio with porous coating (3) increases linearly as the mass flux increases in fig. 9. The maximum increase of CHF using coating (3) (d_p = 30-40 μm) compared to the smooth tube is 71% at the mass flux of 300 kg/m^{2}s in this figure. However, under the same experimental conditions, the CHF with porous coating (4) (d_p = 60-80 μm) is 45% higher than the one in the smooth tube. At the pressure of 0.4 MPa, coating (4) does not show any significant effect on the CHF with the mass flux. However, coating (3) shows a small negative effect for mass fluxes of 50 and 100 kg/m^{2}s, and a small positive effect for mass fluxes of 200 and 300 kg/m^{2}s. At 0.7 MPa, the CHF ratio for coating (4) shows a peak value at 100 kg/m^{2}s; otherwise, there is no visible effect for coating (4). For porous coating (3), at 0.7 MPa, the CHF ratio increases as the mass flux increases up to 100 kg/m^{2}s. Stein [20] reported that there are no measured CHF data for coating (3) for mass fluxes higher than 100 kg/m^{2}s due to inadequate heating power in the experimental set-up.

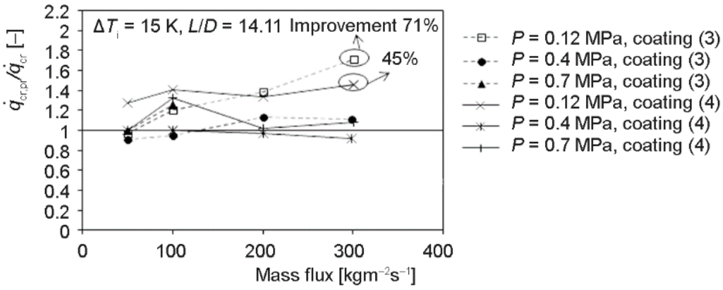

Figure 9. The effect of the mass flux on the CHF with porous coating (3) and (4) for the inlet subcooling of 15 K [20]

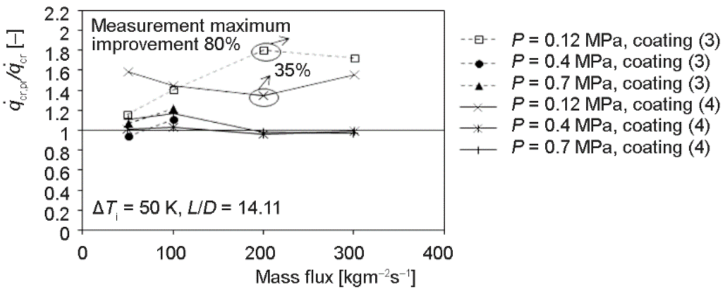

Figure 10. The effect of the mass flux and the pressure on the CHF ratio with porous coating (3) and (4) for the inlet subcooling of 50 K [20]

At the pressure of 0.12 MPa, for the inlet subcooling of 50 K, both coating (3) (except mass flux 50 kg/m^{2}s) and (4) show a significant improvement of the CHF compared to the smooth tube in fig. 10. However, the increase in the CHF with porous coating (3) and (4) is strongly dependent on the mass flux at atmospheric pressure. The CHF on coating (3) (d_p = 30-40 μm) reaches its maximum value, which is 80% for the mass flux of 200 kg/m^{2}s at 0.12 MPa. However, under the same experimental conditions, the CHF with porous coating (4) (d_p = 60-80 μm) is 35% higher than the one in the smooth tube. At elevated pressures, porous coating (3) and (4) do not show any significant effect on the CHF with increasing mass flux.

Stein [20] reported that the CHF for *L/D* = 50 deteriorates with the use of the porous coating (3) and (4) at atmospheric pressure. The deterioration increases with increasing the mass flux for the inlet subcoolings of 30 and 50 K. At elevated pressure, the effect of the porous coating becomes invisible. Table 3 shows the maximum values of the CHF for each porous coating.

Table 3. The effect of the porous coating parameters on the CHF

Porous coating	D [mm]	Length L [mm]	***L/D***	Particle diameter, d_p, [μm]	layer thickness, δ, [μm]	Porosity, ε, %	$\dfrac{\dot{q}_{cr,pr}}{\dot{q}_{cr}}$	Remarks
Coating (3) [20]	9	127	**14.1**	30-40	300	60-75	**1.8**	ΔT_{sub} = 50 K G = 200 kg/m^{2}s P = 0.12 MPa
Coating (4) [20]				60-80			1.35	
Coating (3) [20]	9	127	**14.1**	30-40	300	60-75	1.11	ΔT_{sub} = 50 K G = 50 kg/m^{2}s P = 0.12 MPa
Coating (4) [20]				60-80			**1.58**	
Coating (1) [19]	6	170	**28.3**	80-100	350	60-70	**1.41**	ΔT_{sub} = ~10 K G = 200 kg/m^{2}s P = 0.42 MPa
Coating (2) [19]	8	310	**38.75**	100-140	180	~50	**1.19**	ΔT_{sub} = 30 K G = 100 kg/m^{2}s P = 0.7 MPa

The results show that the effect of the porous coatings on the CHF may be positive, negative, or even neutral depending on the mass flux, pressure, and inlet subcooling. There is a positive effect of porous coatings caused by capillary forces that feed the heated surface with liquid and an increment of the number of nucleation sites. The smaller bubbles on the porous-coated surface with small particle diameter may grow more quickly and bring more liquid replenishment after bubble departure. These effects may result in an increased rate of turbulence, resulting in a higher CHF value. However, a negative effect of porous coating may be expressed as an increased entrainment depending on the coating parameters and the tube length. An increase of entrainment may lead to a decrease of the liquid film on the wall and thus to an earlier drying out of the heating surface.

Conclusions

The CHF depending on the L/D ratio, mass flux, pressure, inlet subcooling, and parameters of the porous coating was investigated. The experiments were carried out during upflow boiling of water in vertical smooth and porous-coated tubes at pressures from 0.11-0.7 MPa, mass fluxes from 50 kg/m^{2}s to 400 kg/m^{2}s, and inlet subcoolings from 1 K to 70 K. This study also took into account the CHF data from the literature. Thus, the range of the L/D ratio was expanded from 14.11 to 50. In general, the CHF decreases with an increase in the L/D ratio for smooth and porous-coated tubes. As the L/D ratio, mass flux, pressure, and subcooling change, the effect of each porous coatings on the CHF changes.

The CHF data for L/D = 14.11 from the literature showed that the CHF with porous coatings is generally higher than in the smooth tube at atmospheric pressure. The improvement of CHF increases with an increase in the inlet subcooling. The maximum improvement of the CHF was 80% with porous coating (3) (having smaller particle diameter) for the mass flux of 200 kg/m^{2}s at inlet subcooling of 50 K at atmospheric pressure. At the same experimental conditions the improvement of the CHF was 35% with porous coating (4) (having larger particale diameter). At elevated pressure, some improvement was observed, but little deterioration or no effect of the porous coating depending on the mass flux and inlet subcooling was observed for porous coating (3) and (4).

The present CHF data for L/D = 28.33 showed that, generally at atmospheric pressure, a deterioration of the CHF with the porous coating (1) was visible in comparison to the smooth tube. At elevated pressure, the CHF increases with coating (1) compared to the smooth tube. The maximum improvement of the CHF with coating (1) was 41% compared to the smooth tube at 0.4 MPa for the mass flux of 200 kg/m^{2}s and for the inlet subcooling of about 10 K. In general, for L/D = 28.33, the improvement of CHF with porous coating was observed at low inlet subcooling at elevated pressures. Otherwise, the effect of the porous coating on CHF was slightly positive, negative, or even neutral.

Acknowledgment

The author would like to thank Dr. Ing. Michael Stein for providing the experimental data.

References

[1] Body, R. D., Subcooled Flow Boiling Critical Heat Flux (CHF) and its Application to Fusion Energy Components, Part 1: A Review of Fundamentals of CHF and Related Database, *Fusion Technology, 7* (1985), 1, pp. 7-30
[2] Incropera, F. P., DeWitt, D. P., *Fundamentals of Heat and Mass Transfer*, 4th ed., John Wiley and Sons, New York, USA, 1996
[3] Celata, G. P., *et al.*, Geometrical Effects on the Subcooled Flow Boiling Critical Heat Flux, *Rev. Gen. Therm., 36* (1997), 11, pp. 807-814
[4] Tanase, A., Improved Methodology for Deriving the Critical Heat Flux Look-Up Table, Master of Applied Science, University of Ottawa, Ottawa, Canada, 2007
[5] Collier, J. G., Thome, J. R., *Convective Boiling and Condensation*, 3rd ed., Oxford University Press, Oxford, UK, 1994
[6] Mastrullo, R., *et al.*, Experimental CHF for Low-GWP Fluids and R134a, Effect of the Lh/D Ratio at Low and High Mass Velocities, *International Journal of Heat and Mass Transfer, 109* (2017), June, pp. 1200-1216
[7] Sudo, Y., Effect of Channel Length on Critical Heat Flux under Conditions of High Subcooling and High Velocity in Short Heated Channels, *Heat Transfer-Japanese Research, 27* (1998), 7, pp. 509-521
[8] Mudawar, L., *et al.*, Ultra-High Critical Heat Fux (CHF) for Subcooled Water Flow Boiling-I: CHF Data and Parametric Effects for Small Diameter Tubes, *International Journal of Heat and Mass Transfers, 42* (1999), 8, pp. 1405-1428
[9] Lee, Y. H., *et al.*, A Correction Method for Heated Length Effect in Critical Heat Flux Prediction, *Nuclear Engineering and Design, 199* (2000), 1-2, pp. 1-11
[10] Roday, A. P., *et al.*, A Review of the Critical Heat Flux Condition in Mini-And Micro-channels, *Journal of Mechanical Science and Technology, 23* (2009), 9, pp. 2529-2547
[11] Wu, Z., *et al.*, A New Predictive Tool for Saturated Critical Heat Flux in Micro/Mini-Channels: Effect of the Heated Length-to-Diameter Ratio, *International Journal of Heat and Mass Transfers, 54* (2011), 13-14, pp. 2880-2889
[12] Kovalev, S.A., *et al.*, Heat Transfer in the Boiling of Water on a Porous Surface in an Annular Channel, *High Temperature, 26* (1988), 5, pp. 918-922
[13] Leont'ev, A. I., *et al.*, Experimemtal Study of Heat-Transfer Burnout in Horizontal Steam – Generating Channels with a Porous Inner Lining and Circumferentially Nonuniform Heating, *High Temperature, 20* (1982), 6, pp. 897-901
[14] Kovalev, S. A., *et al.*, Liquid Boiling on Porous Surfaces, *Heat Transfer-Soviet Research, 19* (1987), 3, pp. 109-120
[15] Kotov, S. A., *et al.*, Burnout in Steam-Generating Channels with Porous Coatings, *High Temperature, 30* (1992), 4, pp. 640-645

[16] Zuev, A. V., *et al.*, Dry-Out Phenomena at Two-Phase Flows in Tubes with Porous Coatings, *Proceedings,* 10th International Heat Transfer Conference, Brighton, UK, 1994, Vol. 6, pp. 147-150
[17] Dawidowicz, B., *et al.*, Heat Transfer and Pressure Drop During Flow Boiling of Pure Refrigerants and Refrigerant/Oil Mixtures in Tube with Porous Coating, *International Journal of Heat and Mass Transfers, 55* (2012), 9-10, pp. 2549-2558
[18] Mel'nikov, V. N., *et al.*, Experimental Study of the Effect of Ferric-Oxide Scale on the Critical Heat Flux in Forced-Convection Boiling of Water, *Heat Transfer-Soviet Research, 11* (1979), 3, pp. 36-39
[19] Yildiz, S., Experimental Investigation of the Critical heat Flow Density in the Transition from DNB to Dry Out Mechanism in Smooth and Porous-Coated Pipes at Low Pressures and Mass Flow Densities (in German), Ph. D. thesis, Koster, Aneich, Germany, Vol. 5, 1998.
[20] Stein, M., Systematic Investigation of the Critical Heat Flux Density at Flow Boiling of Water in Vertical Circular Tubes with and without Porous Coating (in German), Ph. D. thesis, Technical University of Berlin, Berlin, 2004

Paper submitted: April 26, 2019
Paper revised: December 18, 2019
Paper accepted: December 22, 2019